Magnetic Ordering in Relation to the Room-Temperature Magnetoelectric Effect of $Sr_3Co_2Fe_{24}O_{41}$

Minoru Soda, Taishi Ishikura, Hiroyuki Nakamura, Yusuke Wakabayashi, and Tsuyoshi Kimura

Division of Materials Physics, Graduate School of Engineering Science, Osaka University, Toyonaka, Osaka 560-8531, Japan

(Received 19 September 2010; revised manuscript received 7 January 2011; published 22 February 2011)

The origin of a room-temperature magnetoelectric (ME) effect has been examined by means of neutron powder diffraction measurements for a Z-type hexaferrite $Sr_3Co_2Fe_{24}O_{41}$. The temperature and magnetic-field dependence of the electric polarization P and several magnetic Bragg reflections show that a commensurate magnetic order with a (0,0,1) propagation vector has an intimate connection with the ME effect. The room-temperature ME effect can be understood in terms of the appearance of P which is induced by a transverse conical spin structure through the inverse Dzyaloshinskii-Moriya mechanism in analogy with Y-type hexaferrites.

DOI: 10.1103/PhysRevLett.106.087201 PACS numbers: 75.85.+t, 61.05.F−, 75.25.−j, 75.80.+q

In the past decade, there has been a huge revival of interest in multiferroics showing both magnetic and ferroelectric orders simultaneously [1,2]. In a class of multiferroic systems in which ferroelectricity is induced by a noncollinear spin arrangement, the application of a magnetic field H causes a drastic change in electric polarization P, namely, giant magnetoelectric (ME) effects [3]. The operating temperatures and magnetic fields have typically been less than 30 K and more than 1 T, which limits applications in technologies. Very recently, however, it has been discovered that a Z-type hexaferrite $Sr_3Co_2Fe_{24}O_{41}$ (SCFO) shows ME effects even at room temperature by applying a low H [4]. This discovery is important from an application standpoint because the ferroelectricity can be controlled with a small H under ambient temperature T conditions. To point out a route toward generalization of the promising ME effect, it is necessary to clarify the underlying mechanism.

Hexaferrites are classified into several types [5,6], of which the Y-type and the Z-type hexaferrites have been reported as magnetoelectrics [4,7,8]. As drawn in Fig. 1, the Y-type hexaferrite is formed by S- and T-blocks while the Z-type hexaferrite is formed by S-, T-, and R-blocks. For the Y-type hexaferrites, such as $(Sr, Ba)_2Zn_2Fe_{12}O_{22}$, the ME effect can be observed only up to ~110 K [7]. The relationship between the ME effect and the magnetic structure has been well discussed based on neutron diffraction results of single crystal samples of the Y-type hexaferrite [9,10]. These neutron studies reported that the proper-screw or longitudinal conical spin structure changes to the transverse conical structure in which the magnetic unit cell is composed of two large (μ_L) and two small (μ_S) moments by applying H along the c plane, as shown in Fig. 1(a). In the transverse conical structure, finite P can be induced by its cycloidal component in terms of the spin-current or inverse Dzyaloshinskii-Moriya (DM) mechanism [11,12]. Thus, the ME effect in the Y-type hexaferrites has been explained by these mechanisms [8–10]. In the case of the Z-type hexaferrite, no information on the magnetic structure related to the ME effect has been reported to date. Thus, the origin of the ME effect of the Z-type hexaferrite is still unclear. In this study, powder neutron diffraction was carried out over wide T and H ranges on the Z-type hexaferrites $(Sr, Ba)_3Co_2Fe_{24}O_{41}$ to examine the mechanism for the low-field ME effect operating at room temperature. By considering the comparison with the Y-type hexaferrite and the difference between SCFO and $Ba_3Co_2Fe_{24}O_{41}$ (BCFO), we found that both the T and H profiles of the ME effect are closely related to the transverse conical structure with a (0,0,1) propagation vector.

Polycrystalline samples of SCFO and BCFO were prepared by the solid-state reaction [13]. Neutron scattering measurements were carried out on the obtained polycrystalline samples using the ISSP triple axis spectrometers

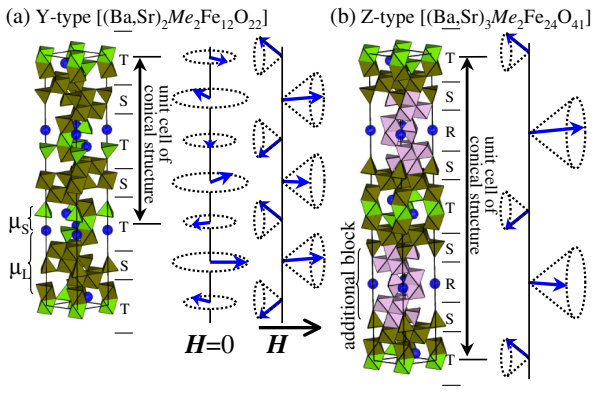

FIG. 1 (color online). Schematic crystal and proposed magnetic structures of (a) Y-type and (b) Z-type hexaferrites. In the Y-type hexaferrite, the proper-screw or longitudinal conical magnetic structure transforms into the transverse conical one which allows finite P by applying H along the c plane [9,10]. When the additional block is inserted into the Y-type hexaferrite, the Z-type structure is obtained.

PONTA and HQR installed at JRR-3 of JAEA, Japan. To compare the neutron scattering results with macroscopic magnetic and ME properties, magnetization M and P were also measured. Details of the experiments are described in Ref. [13].

The first step was to search for T-dependent diffraction peaks in the absence of H. Figure 2(a) shows neutron powder diffraction (NPD) patterns of SCFO measured at $T = 150$ and 566 K. For the data at 566 K, which is below the magnetic ordering temperature ($= 670$ K), a Rietveld analysis [14] was carried out using the space group $P6_3/mmc$ and the ferrimagnetic structure reported by Tachibana and co-workers [15,16]. As shown in Fig. 2(a), the profile at 566 K is well explained by these chemical and magnetic structures. Compared with the NPD profile at 566 K, additional peaks evidently exist at 150 K: $00l_o$ reflections ($l_o =$ odd), which are forbidden in the space group $P6_3/mmc$. In addition, intensities of $00l_e$ Bragg reflections ($l_e =$ even) are enhanced in the profile at 150 K. As shown in the inset of Fig. 2(a), the $00l_o$ reflections appear below 400 K and increase in intensity with decreasing T. Since these additional reflections are not observed in x-ray powder diffraction measured at room temperature [4], we conclude that they are the magnetic reflections characterized by the magnetic propagation vector $\boldsymbol{q}_m = (0, 0, 1)$, indicating that $00l_o$ corresponds with $\pm(0, 0, 1)$ satellite points of $00l_e$.

The magnetic scattering on the $(0, 0, L)$ line and that on the $(1, 0, L)$ line are affected by different components of the magnetic ordering from the magnetic scattering because neutrons are scattered by magnetic moments perpendicular to the scattering vector. The $00L$ and $10L$ magnetic intensities provide the amplitude of the ordered moments parallel to the c plane and to the $(10L)$ plane containing a finite c-axis component, respectively. Here, we focus on the 008 and 009 magnetic reflections to study the in-plane magnetic structure and on the 100, 101, and 102 magnetic reflections observed around $2\theta \simeq 26.5°$ to study the out-of-plane component of the magnetic structure. Since the latter three reflections are too close to each other, we call them "$10L$ peak."

Figure 3(a) shows the T profiles of the peak intensity of the $10L$ peak and the integrated intensities of the 008 and 009 reflections in SCFO measured at $H = 0$. The nuclear components of the $10L$ peak (n_{10L}) and the 008 reflection (n_{008}), which were estimated by the Rietveld analysis for

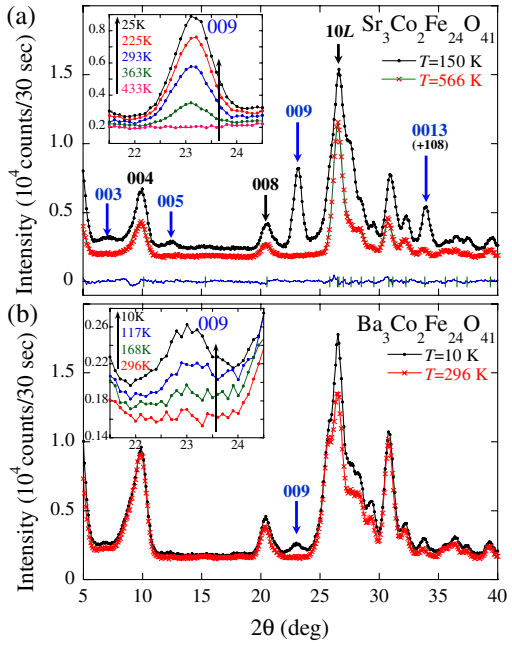

FIG. 2 (color online). Neutron powder diffraction (NPD) patterns of (a) SCFO and (b) BCFO measured at two temperatures. Major Bragg positions are indicated by arrows and indices of the space group $P6_3/mmc$. In the data taken at 566 K of SCFO, the calculated curve obtained by the Rietveld fitting with the space group $P6_3/mmc$ and the ferrimagnetic structure [15,16] is shown by the solid curve. At the bottom of (a), the Bragg positions are indicated by the vertical lines and the difference between the observed and calculated data is also shown. The insets show NPD patterns around the 009 reflection at various temperatures.

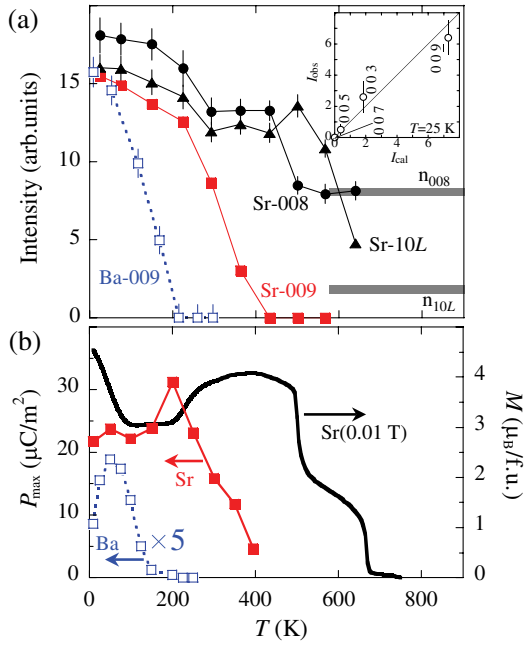

FIG. 3 (color online). (a) T dependence of the peak intensity of the $10L$ peak and the integrated intensities of the 008 and 009 reflections estimated from the neutron profiles of SCFO and BCFO. The nuclear components of the $10L$ peak (n_{10L}) and the 008 reflection (n_{008}) are shown by gray lines. (b) T dependence of M and P_{max} for the polycrystalline samples of SCFO and BCFO. The P_{max} values of BCFO are multiplied by 5 for presentation. Inset: The integrated intensities of the $00l_o$ magnetic reflections observed at 25 K in SCFO are compared with those calculated using the transverse conical structure shown in Fig. 1(b).

the 566 K data, are also shown. As T decreases from 640 to 500 K, the intensity of the 10L peak increases rapidly while the 008 reflection has no change. As T drops from 500 to 430 K, the intensity of 10L decreases slightly and that of 008 increases, showing an increase of the c-plane component of the ordered moment in this T range. In our Rietveld analyses using the ferrimagnetic structures reported in Refs. [15,16], the angles of the moments from the c axis were estimated to be 0.0° and 50.5° at 566 and 460 K, respectively. By considering both the T dependence of M shown in Fig. 3(b) and the neutron intensities, we found that the ferrimagnetic ordering with the moments along the c axis occurs at 670 K with decreasing T and that the magnetic moments are rotated towards the c plane below 500 K. With further decreasing T, the 009 reflection appears below 400 K even though the intensities of the 008 and 10L magnetic reflections remain unchanged, meaning that a new magnetic structure which breaks $P6_3/mmc$ symmetry is established below ~400 K.

To elucidate the effect of H on the magnetic structure which develops below ~400 K, the magnetic reflections of SCFO were measured as a function of H at 10 and 300 K. The results are summarized in Fig. 4(a). As shown in the inset of Fig. 4(a), significant changes in the neutron intensities were observed by applying H. The main panel shows the H dependence of the 008 and 009 integrated intensities as well as the 10L peak intensity at 10 K. The intensities of the 10L and 008 reflections increase with increasing H and are saturated above 3 T. By contrast, the intensity of the 009 reflection decreases and disappears above 3 T, indicating that the magnetic structure having the (0,0,1) propagation vector exists only below 3 T. The integrated intensity of the 009 reflection taken at 300 K up to 0.8 T using the electromagnet is also shown in Fig. 4(a), which demonstrates that the 009 reflection has a similar H dependence even at room temperature.

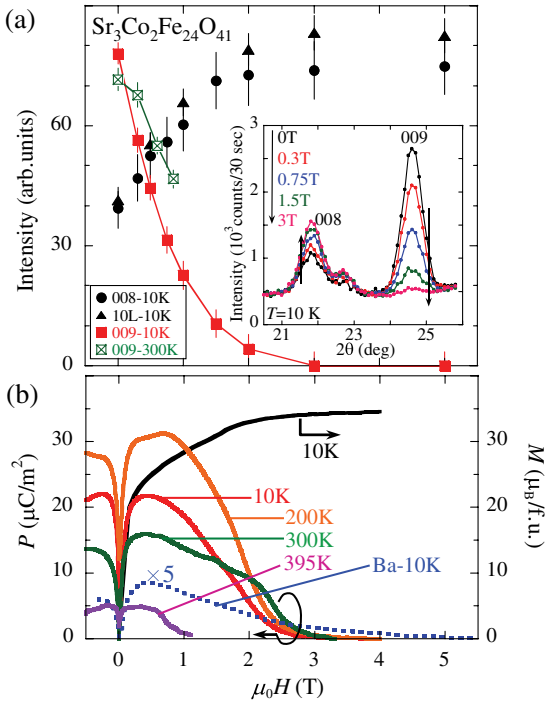

FIG. 4 (color online). (a) H dependence of the peak intensity of the 10L peak and the integrated intensities of the 008 and 009 reflections estimated from the neutron profiles of SCFO. The inset shows the NPD profiles around the 008 and 009 reflections at several magnetic fields. (b) H dependence of M and P for the polycrystalline samples of SCFO and BCFO at several temperatures. The P values of BCFO are multiplied by 5 for presentation.

To clarify the connection between the magnetic ordering and the ME effect in SCFO, we examined the T and H dependence of P. Figure 4(b) shows P as a function of H at several temperatures. At all the temperatures, P develops rapidly by applying H, shows a broad peak structure around 0.5 T, and becomes almost zero above 3 T. Both the critical magnetic field and the magnitude of P are larger than those reported previously [4]. We believe that the change in the postannealing procedure [13] makes the effects on the critical field and the magnitude of P. In fact, it has been reported that the critical field in a ME Y-type $Ba_{0.5}Sr_{1.5}Zn_2Fe_{12}O_{22}$ strongly depends on the annealing procedure [17]. The maximum value P_{max} obtained from the H dependence of P at each T is plotted in Fig. 3(b). The H-induced P, that is, the ME effect, is observed up to 400 K. The T-H regions showing the ME effect coincide with those with finite $00l_o$ magnetic reflections. This correlation is also observed in BCFO. In BCFO, the 009 magnetic Bragg peak is observed only below 200 K [Figs. 2(b) and 3(a)], and finite P was also observed in the same T range [Fig. 3(b)]. Based on these results, we conclude that the magnetic structure characterized by $\boldsymbol{q}_m = (0, 0, 1)$ is the origin of the ME effect in the Z-type hexaferrite system.

As stated in the introduction, some Y-type hexaferrites also show the ME effect [7,8], which is understood as the result of the inverse DM interaction [9,10]. Here, we discuss whether the ME effect in the Z-type hexaferrites is also explained by the same mechanism. In the H-induced ME phase of the Y-type hexaferrites, the magnetic structure is the transverse conical structure with the commensurate propagation vector $(0, 0, 3/2)$ [9,10], as illustrated in the right-hand panel of Fig. 1(a). In this structure, the magnetic moment μ_S, centered at a T-block, forms a phase π from the neighboring μ_S. For the Z-type structure, the similar transverse conical spin structure illustrated in the right-hand panel of Fig. 1(b), that is, the antiphase arrangement of the magnetic moments between neighboring T-blocks, is characterized by $\boldsymbol{q}_m = (0, 0, 1)$. This is because the chemical stacking of the $P6_3/mmc$ Z-type $(ABAB\ldots)$ is different from that of the $R\bar{3}m$ Y-type $(ABCABC\ldots)$. This magnetic structure is also able to produce P through the inverse DM interaction, and the propagation vector is the same as that observed experimentally.

Furthermore, we carried out the magnetic structure analysis. The inset of Fig. 3(a) shows the integrated intensities of the $00l_o$ magnetic reflections observed at 25 K (I_{obs}) with respect to those calculated for the transverse conical structure shown in Fig. 1(b) (I_{cal}). The observed and calculated results agree very well, which indicates that the proposed transverse conical structure is consistent with the experimental result. In addition to the inverse DM mechanism, the symmetric-type magnetostriction may cooperatively contribute to P in the present spin-spiral Z-type hexaferrites, as pointed out in Ref. [18]. However, a detailed theoretical calculation is needed to test such cooperative contributions.

For a system with a conical structure, the cone angle and the easy axis of magnetization are usually changed by applying H. The disappearance of the 009 reflection and the saturation of the 008 reflection above 3 T, which are shown in Fig. 4(a), indicate that the conical structure transforms into a collinear ferrimagnetic structure. This agrees with the H dependence of M shown in Fig. 4(b). In this scenario, the cycloidal component disappears above 3 T, which is also consistent with the disappearance of P above 3 T in the framework of the inverse DM mechanism. Therefore, the inverse DM mechanism through the transverse conical spin structure shown in Fig. 1(b) is the most probable mechanism of the room-temperature ME effect in the Z-type hexaferrite SCFO. This idea is supported by the results on BCFO, in which both the $00l_o$ magnetic Bragg reflections and the electric polarization sustain only up to $\sim$200 K and are almost 1 order of magnitude smaller than those in SCFO. This means that the magnetic frustration which stabilizes the conical structure in BCFO is smaller than that in SCFO. One drawback for the inverse DM interpretation is the suppression of P around $H = 0$, where the $00l_o$ reflections remain intact, as shown in Fig. 4. A similar significant change in P without any change in $\boldsymbol{q}_m$ was also observed in the Y-type hexaferrite, which has been discussed in terms of the rotation of the cycloidal moments [10]. We speculate that the similar moment rotation and/or the formation of magnetic domains occur at very low H.

Finally, let us comment on a possible explanation of why the Z-type SCFO shows the spiral spin order and the resultant magnetoelectric effect at higher T with respect to the Y-type hexaferrites. In Y-type $Ba_{2-x}Sr_xZn_2Fe_{12}O_{22}$, the enhancement of the spiral transition temperature has been discussed in terms of the change in the superexchange interaction between two Fe sites crossing the boundary between blocks forming μ_L and μ_S [19]. Since Ba (or Sr) ions are located near these two Fe sites, the substitution of small Sr for large Ba causes the change in the Fe-O-Fe bond angle ϕ near the boundary (e.g., $\phi = 113°$ in $Ba_2Zn_2Fe_{12}O_{22}$ and $\phi = 118°$ in $Ba_{0.5}Sr_{1.5}Zn_2Fe_{12}O_{22}$) [19]. The increase of ϕ causes the magnetic frustration at the boundary, and then stabilizes a noncollinear spiral spin structure. This discussion can also be applied to the Z-type hexaferrites in which ϕ of BCFO and SCFO is 116° and 123°, respectively [20]. When we compare ϕ between the Z-type SCFO and the Y-type $Ba_{0.5}Sr_{1.5}Zn_2Fe_{12}O_{22}$, the former is larger than the latter by $\sim$5° and may enhance the magnetic frustration. We speculate that this large ϕ of SCFO stabilizes the spiral magnetic order and contributes to its higher magnetoelectric performance. This suggestion will help in designing more advanced ME hexaferrites.

In conclusion, neutron powder diffraction studies were carried out on a Z-type hexaferrite $Sr_3Co_2Fe_{24}O_{41}$ having the room-temperature magnetoelectric effect. We confirmed a close relationship between the magnetic-field-induced electric polarization and the magnetic Bragg reflections with the propagation vector of (0,0,1). The magnetic reflections can be ascribed to a transverse conical spin structure which allows finite polarization in terms of the inverse Dzyaloshinskii-Moriya mechanism. Our results provide a natural explanation of the magnetoelectric effect in the Z-type hexaferrite.

Work at the JRR-3 was supported by ISSP of the University of Tokyo. This work was supported by KAKENHI (19052002, 20674005, and 20740171) and Global COE program (G10).

[1] N. A. Hill, J. Phys. Chem. B **104**, 6694 (2000).
[2] M. Fiebig, J. Phys. D **38**, R123 (2005).
[3] S.-W. Cheong and M. Mostovoy, Nature Mater. **6**, 13 (2007).
[4] Y. Kitagawa *et al.*, Nature Mater. **9**, 797 (2010).
[5] J. Smit and H. P. J. Wijn, *Ferrites* (Philips Technical Library, Eindhoven, The Netherlands, 1959).
[6] P. B. Braun, Philips Res. Rep. **12**, 491 (1957).
[7] T. Kimura, G. Lawes, and A. P. Ramirez, Phys. Rev. Lett. **94**, 137201 (2005).
[8] S. Ishiwata *et al.*, Science **319**, 1643 (2008).
[9] H. Sagayama *et al.*, Phys. Rev. B **80**, 180419(R) (2009).
[10] S. Ishiwata *et al.*, Phys. Rev. B **81**, 174418 (2010).
[11] H. Katsura, N. Nagaosa, and A. V. Balatsky, Phys. Rev. Lett. **95**, 057205 (2005).
[12] I. A. Sergienko and E. Dagotto, Phys. Rev. B **73**, 094434 (2006).
[13] See supplemental material at http://link.aps.org/supplemental/10.1103/PhysRevLett.106.087201 for the details of the sample preparation and the measurements.
[14] F. Izumi and T. Ikeda, Mater. Sci. Forum **321–324**, 198 (2000).
[15] T. Tachibana *et al.*, J. Magn. Magn. Mater. **262**, 248 (2003).
[16] Y. Takada *et al.*, J. Appl. Phys. **100**, 043904 (2006).
[17] Y. S. Chai *et al.*, New J. Phys. **11**, 073030 (2009).
[18] M. Mochizuki, N. Furukawa, and N. Nagaosa, Phys. Rev. Lett. **105**, 037205 (2010).
[19] S. Utsumi, D. Yoshiba, and N. Momozawa, J. Phys. Soc. Jpn. **76**, 034704 (2007).
[20] Y. Takada *et al.*, J. Jpn. Soc. Powder Powder Metall. **50**, 618 (2003).